Organic & Biomolecular Chemistry

PAPER

View Article Online
View Journal

Cite this: DOI: 10.1039/c7ob01312d

C–ON bond homolysis of alkoxyamines: when too high polarity is detrimental†

Paulin Nkolo,[a] Gérard Audran,*[a] Raphael Bikanga,[b] Paul Brémond,[a] Sylvain R. A. Marque *[a,c] and Valérie Roubaud[a]

Throughout the last decade, the effect of electron withdrawing groups (EWGs) has been known to play a role – minor or moderate depending on the nitroxyl fragment R_1R_2NO – in the change in the homolysis rate constant (k_d) for C–ON bond homolysis in alkoxyamines (R_1R_2NOR). It has been shown that the effect of EWGs on k_d is described by a linear relationship with the electrical Hammett constant σ_I. Since then, linear multi-parameter relationships $f(\sigma_{RS},\nu,\sigma_I)$ have been developed to account for the effects involved in the changes in k_d, which are the stabilization of the released radical (σ_{RS}) and the bulkiness (ν) and polarity (σ_I) of the alkyl fragment. Since a decade ago, new results have been published highlighting the limits of such correlations. In this article, previous multi-parameter linear relationships are amended using a parabolic model, *i.e.* $(\sigma_{I,nitroxide} - \sigma_{I,alkyl})^2$, to describe the effect of EWGs in the alkyl fragment on k_d. In contrast to previous studies, these improved linear multi-parameter relationships $f(\sigma_{RS},\nu,\Delta\sigma_I^2)$ are able to account for the presence of several EWGs on the alkyl fragment, R. An unexpectedly strong solvent effect – a *ca.* 1500-fold increase in k_d – from *tert*-butylbenzene to the water/methanol mixture is also observed for 3-((2,2,6,6-tetramethylpiperidin-1-yl)oxyl)pentane-2,4-dione **1b** in comparison to a *ca.* 5-fold increase in k_d that is generally observed.

Received 29th May 2017,
Accepted 16th June 2017

DOI: 10.1039/c7ob01312d

rsc.li/obc

Introduction

In the last few years,[1] the cleavage/reformation property of alkoxyamines, affording an unexpectedly long lifetime for this species, has been implemented in various applications such as self-healing polymers,[2,3] materials for photonics,[4] and coding systems.[5,6] Recently, the external triggering of the C–ON bond in alkoxyamines was used to highlight[7] the potential use of these molecules as agents for Theranostics.[8] For three decades, alkoxyamines had been used as initiators/controllers in Nitroxide Mediated Polymerization.[9] Today, restrictive regulations encourage the development of more efficient and more secure initiators.[10] Hence, all these new developments require the accurate and reliable knowledge of the factors controlling the C–ON bond homolysis, both to design new efficient molecules and to get deeper insight into the reactivity of these molecules. In the last decade, empirical and theoretical models[11,12] have been developed to account for the different effects that influence the rate constant (k_d) of the C–ON bond homolysis in alkoxyamines (Scheme 1) as well as to drive the design of new alkoxyamines that exhibit the best efficiency for various applications.[1–8] Hence, several empirical multiparameter equations based on different types of Hammett or Taft constants have been developed to account for the effects observed in the nitroxyl and the alkyl fragments.[13,14] Thus, in eqn (1),‡ electrical Hammett constant σ_I describes the effect of electron withdrawing groups (EWGs) on both the stabilization of the released nitroxide and the change in polarity in the alkoxyamine, and E_s accounts for the bulkiness of the nitroxyl fragment.§ For the alkyl fragment,[15] two equations are developed depending on the nitroxyl fragment: eqn (2)¶ for **1**$^\bullet$ (so-called TEMPO)‖ and eqn (3)** for **2**$^\bullet$ (so-called SG1)‖ as released nitroxides – σ_{RS} to account for the

[a]*Aix Marseille Univ, CNRS, ICR, UMR 7273, case 551, Avenue Escadrille Normandie-Niemen, 13397 Marseille Cedex 20, France. E-mail: sylvain.marque@univ-amu.fr, g.audran@univ-amu.fr*

[b]*Laboratoire de Substances Naturelles et de Synthèse Organométalliques Université des Sciences et Techniques de Masuku, B.P. 943, Franceville, Gabon*

[c]*N. N. Vorozhtsov Novosibirsk Institute of Organic Chemistry SB RAS, Pr. Lavrentjeva 9, 630090 Novosibirsk, Russia*

†Electronic supplementary information (ESI) available. See DOI: 10.1039/c7ob01312d

‡ $N = 239$, $R^2 = 0.95$, $t = 99.99\%$, $F_{0.01} = 210$. See ref. 13.

§ This relationship was only developed for the released radical **h**$^\bullet$.

¶ $N = 14$, $R^2 = 0.96$, for ρ_{RS} and δ, $t = 99.99\%$, for ρ_I, $t = 99.45\%$ and $F_{0.01} = 80$. See ref. 15.

‖ $N = 19$, $R^2 = 0.85$, $t = 99.99\%$, $F_{0.01} = 29$. See ref. 15.

** In ref. 15, alkoxyamines are distributed into two families: one for nitroxyl fragments carrying weak EWGs or EDGs with **1**-based alkoxyamines as representatives, and one for nitroxyl fragments carrying EWGs with **2**-based alkoxyamines as representatives.

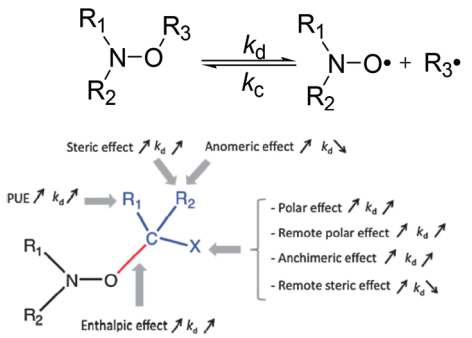

Scheme 1 Different effects that play roles in the changes in k_d. Reproduced by permission of the Royal Society of Chemistry (see ref. 15).

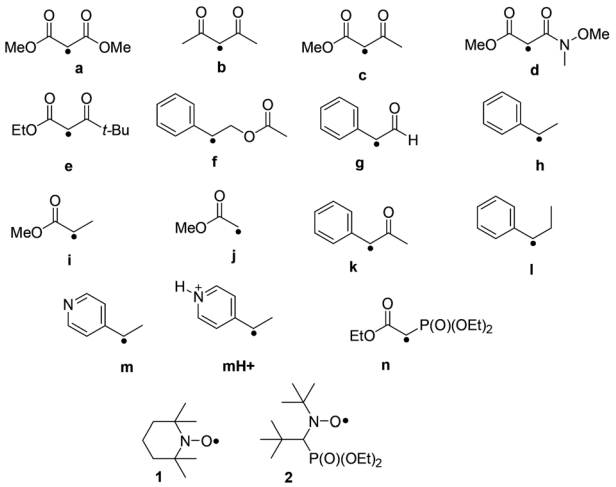

Fig. 1 The alkyl radicals and nitroxides discussed.

stabilization of the released radical, σ_I for the effect of EWG and ν for the bulkiness of the alkyl fragment.

$$\log(k_d/s^{-1}) = -5.88(\pm0.28) - 3.07(\pm0.28)\cdot\sigma_I - 0.88(\pm0.04)\cdot E_s \quad (1)$$

$$\log(k_d/s^{-1}) = -14.8(\pm0.7) + 13.9(\pm0.9)\cdot\sigma_{RS} + 13.6(\pm3.2)\cdot\sigma_I + 6.6(\pm0.7)\cdot\nu \quad (2)$$

$$\log(k_d/s^{-1}) = -14.3(\pm1.3) + 15.3(\pm2.2)\cdot\sigma_{RS} + 19.5(\pm3.0)\cdot\sigma_I + 7.0(\pm1.1)\cdot\nu \quad (3)$$

These correlations were developed with more than 15 k_d values each. It was shown that k_d increases with increasing stabilization of the released radical and with an increase in both the polarity and bulkiness of the substituents $R_{1,2}$ and X (Scheme 1).[16] The robustness, accuracy, and reliability of eqn (2) and (3) have been tested over the years.[17,18] However, some years ago, Studer and coll.[19] reported the reactivity of **1a**, **1e** and **1d** (Fig. 1) and observed higher homolysis activation energies E_a (Table 1) than expected from eqn (2). Taking into account the aforementioned requirements, this led us to thoroughly investigate the polar effect of the alkyl fragment with 7 new alkoxyamines **1a–c,f,g**, and **2a–c** (Fig. 1), which all carry polar alkyl fragments and release stabilized radicals. Their k_d values were measured in *tert*-butylbenzene and in a water/MeOH mixture. The results showed an overestimated polar effect for the TEMPO-based fragment carrying only electron donor groups (EDGs) and a rather good estimate of the polar effect for the SG1-based fragment carrying EWGs. DFT calculations were performed to get deeper insight into how the polarity of the nitroxide influences the polar effect of the alkyl fragment.

Results

Preparation of 1a–c,f,g,m and 2a–c

Alkoxyamine **1m** was prepared as reported for **2m** using nitroxide **1**• as a alkyl radical scavenger.[20,21] Alkoxyamine **1a** was prepared as already reported.[22] Alkoxyamines **1b,c** and **2a–c** (Scheme 2) were prepared by scavenging the alkyl radicals **a**•**–c**• in the presence of nitroxides **1**• and **2**•, respectively. Radicals **a**•**–c**• were generated by oxidation of the anions of malonic acid derivatives in the presence of $CuCl_2$, which were prepared using lithium diisopropylamine (LDA) as a base. Yields ranged from poor (*ca.* 20% for **2**-based alkoxyamines) to moderate (*ca.* 70% for **1**-based alkoxyamines).[22] Moreover, alkoxyamine **2b** was only detected at low temperatures and it decomposed upon warming to room temperature.

Hydrobromination of styrene oxide afforded the expected bromohydrin.[23] The latter, using the Atom Transfer Radical Addition (ATRA) procedure in the presence of **1**•,[24] was transformed into the corresponding alkoxyamine.[25] After purification, the alkoxyamine was oxidized[26] into **1g** or was transformed[25] into **1f** in the presence of acetic anhydride (Scheme 3).

Kinetic measurements

The values of k_d were measured by EPR and used O_2 as the alkyl radical scavenger, as previously reported (Fig. 1SI†).[27] Except for **1a** and **1c** – for which the plateau was not reached due to an excessively long experiment time†† – and for **2b** – which was not stable enough to be handled at room temperature – the plateau of the concentration of nitroxide was reached at the expected level for all of the other alkoxyamines (Table 1). The values of k_d for alkoxyamines **1a**, **1d**, and **1e** have been measured by Studer and coll.[19] A difference of *ca.* 6 kJ mol^{-1} for **1a** cannot be accounted for so far. Alkoxyamines **1k** and **1l** have been measured by Megiel *et al.*[28] in acetonitrile. A difference of *ca.* 7 kJ mol^{-1} between **1g** and **1k** cannot be thoroughly rationalized, because the same stabilization is expected for radicals **g**• and **k**•‡‡ as their polarity is the same

†† In such cases, the initial slope method was used. See ref. 27.

‡‡ $a_{H\alpha}$ = 19.0 G for $HCOCH_2$ and $a_{H\alpha}$ = 19.5 G for $MeCOCH_2$, meaning that these two radicals are similarly stabilized. Thus, it is assumed that $\sigma_{RS,g\cdot} \approx \sigma_{RS,k\cdot}$ or is slightly lower.

Table 1 Experimental C–ON bond homolysis rate constant k'_d at temperature T, activation energy E_a (kJ mol^{-1}) and corresponding k_d at 120 °C

Alkoxyamines	Solvent	T (°C)	k'_d (10^{-4} s^{-1})	E_a	k_d (120 °C in s^{-1})	Ref.[a]
1a	*t*-BuPh	160	6.2	145.8	10^{-5}	t.w.
	t-BuPh			140.0	6×10^{-5}	19
1b	*t*-BuPh	150	3.1	144.9	1.3×10^{-5}	t.w.
1c	*t*-BuPh	150	15.1	139.3	7.3×10^{-5}	t.w.
1d	*t*-BuPh			137.7	1.2×10^{-4}	19
1e	*t*-BuPh			132.1	6.6×10^{-4}	19
1f	*t*-BuPh	130	0.98	131.1	9.0×10^{-4}	t.w.
1g	*t*-BuPh	70	0.76	121.5	0.017	t.w.
1h	*t*-BuPh			132.9	5.2×10^{-4}	27
1i	*t*-BuPh			141.8	3.4×10^{-5}	27
1j	*t*-BuPh			161.5	8.2×10^{-8}	27
1k	Acetonitrile			114.0[b]	0.17	28
1l	Acetonitrile			132.4[b]	6.1×10^{-4}	28
1m	*t*-BuPh	131	34.9	130.3	1.1×10^{-3}	t.w
1mH+	*t*-BuPh[c]	100	5.3	126.1	4.2×10^{-3}	t.w.
2a	*t*-BuPh	110	31.3	123.8	0.008	t.w.
2b	*t*-BuPh		Degradation at −30 °C			n.d.
2c	*t*-BuPh	80	6.0/14.0	118.9/116.4	0.037/0.081	t.w.
2h	*t*-BuPh			125.0/126.4	5.8×10^{-3}/3.8×10^{-3}	27
2i	*t*-BuPh			128.4/130.8	2.1×10^{-3}/10^{-3}	27
2j	*t*-BuPh			149.1	3.6×10^{-6}	27
2m	*t*-BuPh			123.0	0.01	20 and 21
2mH+	*t*-BuPh			115.6	0.1	20 and 21
1a	H_2O/MeOH[d]	80	0.58	125.8	4.6×10^{-3}	t.w.
1b	H_2O/MeOH[d]	80	4.8	121.2	0.019	t.w.
1c	H_2O/MeOH[d]	80	2.4	121.6	1.6×10^{-2}	t.w.
1g	H_2O/MeOH[d]	80	1.80	122.4	0.013	t.w.
1m	H_2O/MeOH[d,e]	81	0.44	127.1	3.0×10^{-3}	t.w
1mH+[f]	H_2O/MeOH[d,g]	81	3.4	121.0	2.0×10^{-2}	t.w.
2a	H_2O/MeOH[d]	80	0.6	119.1	0.035	t.w.
2c	H_2O/MeOH[d]	70	9.0/14.4	114.4/113.1	0.149/0.222	t.w.
2h	H_2O/MeOH[d]			124.0/123.0	7.9×10^{-3}/0.011	30
2m	H_2O/MeOH[d]			119.2/119.4	3.4×10^{-2}/3.2×10^{-2}	32
2mH+	H_2O/MeOH[d,g]			109.7/108.3	0.63/0.97	31

[a] t.w. = this work and n.d. = not determined. [b] Values reported in acetonitrile. Original rate constants were divided by a factor of 2 to account for the solvent effect. See ref. 27 and 29. [c] Protonation was performed *in situ* in the presence of 2 equivalents of TFA. See the ESI† for the ^{1}H NMR signals. [d] MeOH/H_2O 1 : 1 v/v. [e] pH = 7.0. [f] pK_a = 4.22, see the ESI.† [g] pH = 2.0.

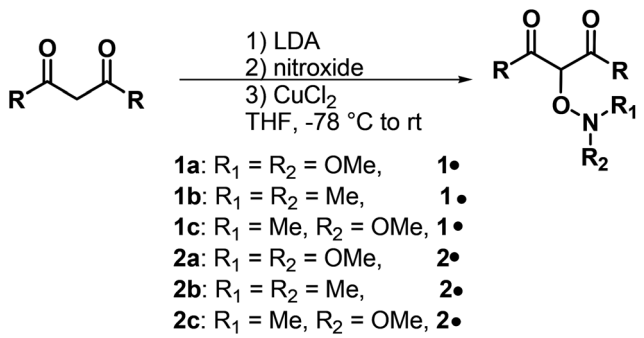

Scheme 2 Preparation of **1a–c** and **2a–c**.

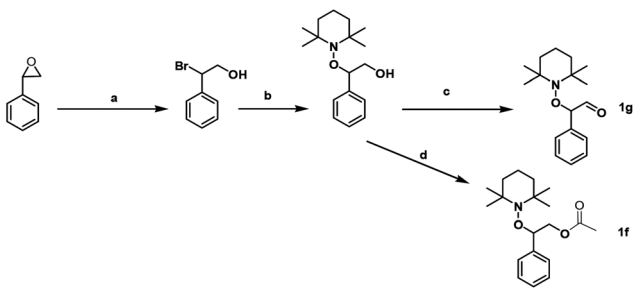

Scheme 3 Preparation of **1f** and **1g**. (a) 47% HBr (aq), $CHCl_3$, 30 min, rt; (b) CuBr/Cu(0)/PMDETA, benzene, 12 h, rt; (c) TPAP, NMO, CH_2Cl_2, 2 h, 0 °C; (d) Ac_2O, Et_3N, CH_2Cl_2, 8 h, rt.

and their bulkiness is not expected to differ too much (*vide infra*).§§ The solvent effect was taken into account as $k_{d,acetonitrile}/k_{d,tBuPh} = 2$.[27,29] As alkoxyamines exhibit interesting potential for application as agents for theranostics, the k_d values were also measured in a water/MeOH (v/v 1 : 1) mixture.[30] Whatever the solvent, diastereoisomers of **2c**¶¶ only exhibit a difference of 1–2 kJ mol^{-1} – a difference already

§§ The k_d value for **1k** has been measured in acetonitrile (see ref. 28). The few data available for type-**1** alkoxyamines have been obtained using weakly polar alkoxyamines. Thus, an unexpected moderate/strong solvent effect cannot be straightforwardly disregarded.

¶¶ As **2c** is an oil, X-ray analysis was not performed and the configurations were not determined.

reported many times for diastereoisomers – and do not deserve further comment.

Multi-parameter relationships

Parameters ν,[33] σ_{RSE},[34,35] and σ_I[36,37] were estimated as previously reported[15] and are shown in Table 1SI.† ||| The coefficients in eqn (2) were re-estimated using ν = 0.58 for CH_2COOMe,[33] $\nu_1 = \nu_{iPr}$ = 0.76 for $CHCH_3COOMe$, $\nu_1 = \nu_{tBu}$ = 1.24 for CMe_2COOMe, and ν_{COOMe} = 0.5,[33] affording $\nu_{CHMeCOOMe}$ = 0.83 and ν_{CMe_2COOMe} = 1.25. Therefore, through using these new values and implementing **1f** and **1l** in eqn (2), which are expected to be included in the correlation, very good statistical outputs (eqn (4))*** were obtained, supporting our new assumptions (Fig. 2). The weight of each effect was estimated as previously reported[15] and afforded 39%, 20%, and 41% for the stabilization, polar, and steric effects, respectively. These values are very close to those previously reported (44%, 16%, and 40%, respectively)[15] and do not deserve further comment.

$$\log(k_d/s^{-1}) = -14.8(\pm0.4) + 12.4(\pm0.9)\cdot\sigma_{RSE} + 17.7(\pm2.2)\cdot\sigma_I + 7.1(\pm0.5)\cdot\nu \quad (4)$$

In the case of homolysis, the activation energy E_a is very similar to the Bond Dissociation Energy (BDE) which depends on the enthalpic and polar terms, as proposed by Pauling[38–40] (eqn (5)). The polar term is given by the square of the difference in electronegativity χ.

Hence, as $\log k_d$ is proportional to E_a – and consequently to the BDE – it has to be proportional to $(\chi_O - \chi_C)^2$ which describes the effect of the changes in polarity in eqn (5).

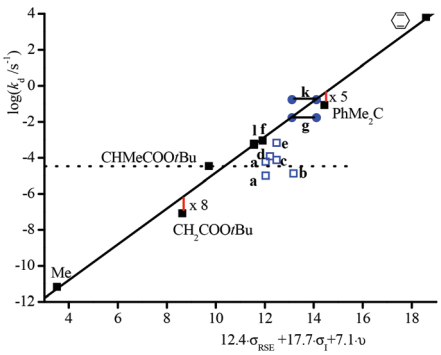

Fig. 2 A plot of $\log(k_d/s^{-1})$ *vs.* $f(\sigma_{RSE},\sigma_I,\nu)$. (■) represents the **1**-based alkoxyamines used in eqn (4) with the extrema displayed; the most deviating data included in the correlation are highlighted by the vertical red lines; (●) represents *k* and *g* for which a range of parameters was defined (horizontal black lines), and (□) represents outlying data.

||| The parameters σ_{RS}, ν, and σ_I were used to account for the effect of the stabilization of the released alkyl radical, the steric hindrance in alkoxyamines due to the bulkiness of the alkyl fragment, and the electron donating or electron withdrawing properties of the EDGs and EWGs, respectively, on k_d. More details are provided in the ESI.†

*** R^2 = 0.98, s = 0.51, N = 16, $F_{99.99\%}$ = 202, and t = 99.99% for all coefficients.

However, it was assumed that changes in the electronegativity of the alkyl fragment, *i.e.*, changes in χ_C, are described by the electrical Hammett constant σ_I (eqn (4)). Therefore, a plot of σ_I *vs.* $\log k_d$ is equivalent to the plot of χ_C *vs.* $(\chi_O - \chi_C)^2$which has a parabolic shape ($y = x^2$) as displayed in Fig. 3. Assuming a nitroxyl fragment carrying a strong EWG for χ_C at position **A** (Fig. 3), a large $(\chi_O - \chi_C)^2$ value and hence a low k_d value are observed. Then, moving to position **B** (increasing χ_C by increasing the polarity), $(\chi_O - \chi_C)^2$ decreases and hence k_d increases linearly (red slope in Fig. 3) due to the shape of the curve. Assuming a nitroxyl fragment with EDGs, the parabolic shape is expected to flatten and is described by the violet line in the case of eqn (2) and by dotted green lines and positions **C–E** in Fig. 3. Thus, for χ_C at position **C**, a small difference in $(\chi_O - \chi_C)^2$ is observed, and, moving to position **D**, $(\chi_O - \chi_C)^2$ decreases only a little, affording a small increase in k_d (purple slope in Fig. 3), and moving further to position **E**, the predicted polar effect is more important than observed, *i.e.*, the purple line is below the parabolic curve.

$$BDE(A-B) = \frac{1}{2}(BDE(A-A) + BDE(B-B)) + a(\chi_A - \chi_B)^2 \quad (5)$$

DFT calculations

To get deeper insight into the polar effect involved in the changes in k_d, DFT calculations were performed for **1a** and **2a** in water and toluene as solvents at the M062X/6-31+G(d,p) level of theory. The PCM standard calculations method has been used for calculations in solvents.[41] Typical bond lengths, distances and angles are reported in Table 2SI† and do not differ from those reported for the molecules in the same family. The dihedral angles θ_1–θ_3 (as well as the θ'_1–θ'_3 needed for their estimations, Fig. 4) for the interactions required at the TS (*vide infra*) are reported in Table 2. The atoms that are involved in dihedral angles θ are displayed in Fig. 4. Angle θ_1 was chosen as the smallest value to reach 90° (*vide infra*), θ_2 for the second ester moiety, and θ_3 to describe the position of the alkyl fragment.

Calculated ΔH_r and $\Delta\Delta H_r$ values are different to the experimental E_a and ΔE_a values (see ESI†) but the trends are the same. Consequently, the calculations and the subsequent parameters reliably describe the reactivity observed for **1a** and

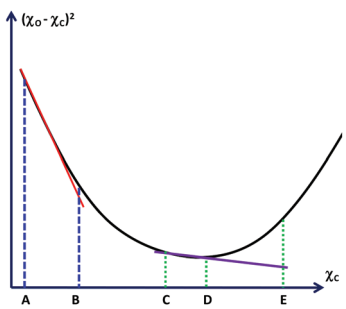

Fig. 3 Parabolic display of the polar effect.

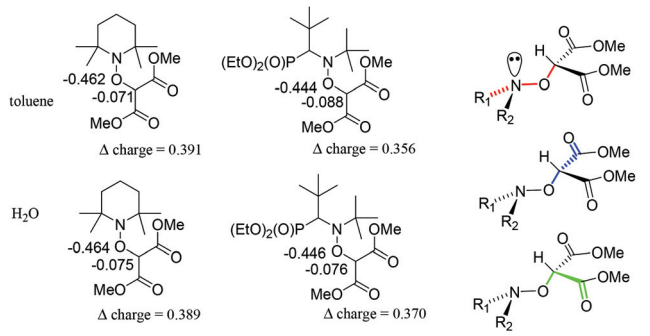

Fig. 4 NBO charge distributions on the O atom of the nitroxyl moiety and on the methine carbon in **1a** (left) and **2a** (right), in water and toluene as solvents. The red, blue, and green colours highlight the dihedral angles θ'_1, θ'_2 and θ'_3, respectively.

Table 2 Geometrical parameters[a] for **1a** and **2a** for the angles required in the TS: θ_1 (dihedral angle $\sigma_{O-C}\pi^*_{C1=O1}$), θ_2 (dihedral angle $\sigma_{O-C}\pi^*_{C2=O2}$), θ_3 (dihedral angle $LP\sigma^*_{O-C}$) and the calculated complementary dihedral angles θ'_1, θ'_2, and θ'_3

	1a		**2a**	
Solvent	Toluene	Water	Toluene	Water
θ'_1 (<OCC_1O_1>)	114	114	52	31
θ_1[b]	24	24	38	59
θ'_2 (<OCC_2O_2>)	173	174	14	26
θ_2[c]	83	84	76	64
θ'_3 (<CNOC>)	128	129	113	127
θ_3[d]	8	9	8	−8

[a] In degrees. Calculated by DFT at the M062X/6-31+G(d,p) level of theory. The solvent effect was estimated using the PCM method. The numbering is displayed in Fig. 4. [b] $\theta_1 = |\theta'_1 - 90°|$. [c] $\theta_2 = |\theta'_2 - 90°|$. [d] $\theta_3 = \theta'_3 - 120°$.

2a qualitatively, in water as well as in toluene. Thus, some interactions that result in stabilization at the TS and a difference in the conformation of the TS with respect to the starting materials are poorly accounted for by the calculated reaction enthalpy.

The NBO charges calculated for **1a** and **2a** in toluene (Fig. 4) show a larger difference (Δ) for **1a** than for **2a**, denoting a larger difference in the electronegativity (χ) between the C and O atoms in **1a** than that in **2a**. A smaller difference is observed in water (Fig. 4), *i.e.*, $\delta\Delta = 0.035$ in toluene and $\delta\Delta = 0.019$ in water, meaning that the stabilization of the polar carbonyl moieties in water decreases the electronegativity of the C atom, leading to an increase in Δ. No significant difference in the Radical Stabilization Energy (RSE) was observed when changing the solvent (see ESI†).

Dipole moments, charges at the proton of the methine carbon in the alkyl fragment and energies E for bonding → anti-bonding orbital interactions in the alkyl fragments are reported for **1a** and **2a** in Table 3SI.† Geometrical parameters (distances and valence angles) for intramolecular H-bonding (IHB) are reported in Table 3SI† for **1a** and **2a**.

Discussion

Studer and coll.[19] reported k_d values for **1a** and **1d** that are very close to those for **1i**, although the methyl group was replaced by the more polar and stabilizing EWGs COOEt and CON(OMe)Me (Table 1SI† and dotted line in Fig. 2). This puzzling result led us to re-investigate the stabilization and polar and steric effects of **1a–c,f,g,m** and **2a,c** which carry groups with very different polarities. Interestingly, k_d values for **1a–e** are estimated by eqn (4) and are 180-, 1500-, 64-, 21- and 7-times larger than when experimentally observed!††† All of these k_d values are clearly lower than expected, meaning that the polar, steric and stabilization effects are not properly described by their respective parameters. The stabilization parameter σ_{RS} is estimated from hyperfine coupling constants and the polar parameter is given by well tabulated Hammett constants σ_I. On the other hand, the steric parameter ν is estimated using several assumptions (*vide supra*). However, no realistic assumptions can account for the large difference that is observed.†††

In sharp contrast to what happens for type-**1** alkoxyamines, the predicted and the experimental values of E_a for **2c** differ by less than 1 kJ mol^{-1}; **2b** decomposes spontaneously despite having an E_a value estimated at *ca.* 108 kJ mol^{-1}, meaning that the bulkiness of **b** is likely to be underestimated, and the E_a for **2a** is 5 kJ mol^{-1} – not 10 kJ mol^{-1} as expected – lower than that for **2i**.‡‡‡ Thus, eqn (3) provides a better description of the effects involved in the C–ON bond homolysis in type-**2** alkoxyamines than eqn (2) does for type-**1** alkoxyamines.

As shown by the DFT calculations, the difference in the charge distribution is larger in **1a** than in **2a**, meaning that the difference in electronegativity χ between the O and C atoms of the C–ON bond is larger in **1a** than in **2a**. In our case, this difference in charges highlights the difference in $(\chi_O - \chi_C)^2$ of the C–ON bond and is accounted for by the Hammett constant σ_I. As the nitroxyl fragment **2** carries strong EWGs ($\sigma_I = 0.28$),[13] changes in k_d are described by positions **A** and **B** in Fig. 3 and eqn (3) holds true, *i.e.* it is a linear description of the polar effect. In contrast, for the nitroxyl fragment **1**, which does not carry EWGs ($\sigma_I = -0.06$),[13] the change in k_d, *i.e.*, the large difference in electronegativity, is described by positions **C** and **E** in Fig. 3 and it is eqn (6) that is valid instead of eqn (2).

It is clear that these two examples describe the polar effect observed in type-**1** and type-**2** alkoxyamines: a strong polar effect (red slope and dashed lines in Fig. 3) occurs for type-**2** alkoxyamines, due to the presence of EWGs on the nitroxyl fragment, described by a linear change in k_d and is well predicted for a broad range of values of σ_I, and a weak polar effect (purple slope and dotted lines in Fig. 3) occurs for type-**1** alkoxyamines, due to the presence of EDGs on the nitroxyl

††† Assuming CO(OMe), Ac, CO(N(OMe)Me) and CO*t*-Bu groups are as sterically demanding as an H atom, $\nu_{CH_2Ac} = 0.76$ for **a**•, **b**•, **c**•, and **e**•. Except for **1e**, which lies on the correlation line, the others are clearly downward outliers.

‡‡‡ This difference might be due to a conformational effect as the conformations of **1i** and **2i** are different.

fragment, described by a linear change in k_d on a very narrow range of σ_I values.

This claim is nicely supported by the E_a for **2mH+** being smaller by *ca.* 8 kJ mol^{-1} (ref. 20 and 21) (*i.e.* a 10-fold increase in k_d) than that for **2m** (going from A to B in Fig. 3), whereas the E_a for **1mH+** is only *ca.* 4 kJ mol^{-1} (*i.e.* a 4-fold increase in k_d, Table 1) smaller than the E_a for **1m** (going from C to D in Fig. 3). Keeping in mind that the protonation of **m** does not change the stabilization of **mH+**$^{\bullet}$ nor the steric demand in **mH+**, as this protonation is performed at the *para* position of the pyridyl ring;[20] changes in k_d are only caused by changes in polarity. Thus, due to the parabolic change in electronegativity as described above, the polar effect is clearly weaker in type-**1** alkoxyamines than in type-**2** alkoxyamines.

Taking these results into account and based on reasonable assumptions,§§§ the data gathered in Table 1 combined with the data reported in the literature are fitted with eqn (6) (Fig. 5). Except for **1k**¶¶¶ and **1b**,‖‖‖‖ which are outliers, all of the other data reported in Table 1 are nicely accounted for by eqn (6) **** (Fig. 5), in sharp contrast to the poor efficiency of eqn (4) (Fig. 2). As expected, the coefficient for the polar effect is negative, meaning the smaller $(\sigma_{I,TEMPO} - \sigma_I)^2$ is, the higher k_d is.

$$\log(k_d/s^{-1}) = -12.2(\pm0.4) + 11.4(\pm0.9)\cdot\sigma_{RS} - 95.0(\pm0.9)\cdot(\sigma_{I,TEMPO} - \sigma_I)^2 + 7.0(\pm0.5)\cdot\nu \quad (6)$$

The values of E_a for **1a–c** decrease dramatically by around 20 kJ mol^{-1} (Table 1) when the solvent is changed from *tert*-butylbenzene to water/MeOH, whereas no change (*ca.* 1 kJ mol^{-1}) is observed for **1g**. The role of the solvent is to stabilize the reactant, products, and transition state (TS). As the homolysis displays the late TS, *i.e.*, it is product-like, any stabilization of the products affords the stabilization of the TS. The polar effect destabilizes the reactant (alkoxyamine), thereby decreasing E_a. The insignificant changes in E_a for **1g** and **2h** (Table 1) when changing the solvent from *t*-BuPh to water/MeOH show that the stabilization of the nitroxide and alkyl radicals due to solvent effects is not strong enough to overbalance the solvation of the alkoxyamine. Moreover, the DFT calculations showed that the solvent effect on the RSE (see the ESI†) can be disregarded. On the other hand, calculations show significant charge separations in the heteronuclear O–C bond (Fig. 4) due to the presence of strong EWGs on the alkyl fragment. Consequently, a polar TS is expected (Fig. 6a) to be more stabilized in water than in a non-polar solvent such as *t*-BuPh, partly accounting for the striking *ca.* 20 kJ mol^{-1} decrease observed in the E_a for **1a**. The same effect should be expected for **2a**, however, a strikingly lower effect is observed, *i.e.*, only a decrease of 4.7 kJ mol^{-1} in E_a.

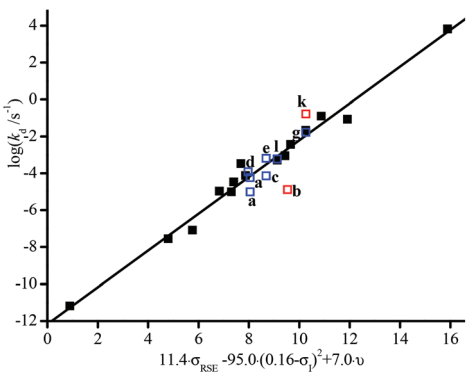

Fig. 5 A plot of $\log(k_d/s^{-1})$ *vs.* $f(\sigma_{RSE},f(\sigma_I),\nu)$. (■) represents **1**-based alkoxyamines used in eqn (6), (□, blue empty square) represents new alkoxyamines and (□, red empty square) represents outlying data.

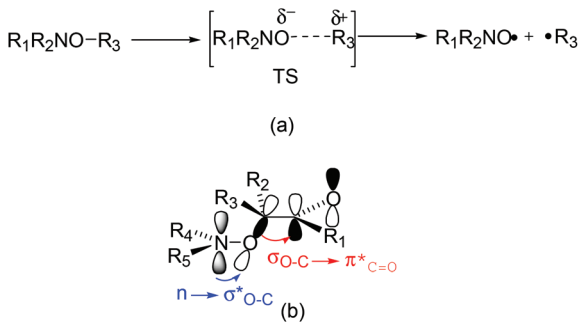

Fig. 6 (a) The charge distribution for a polar TS. (b) The orbital interactions in the expected TS for the homolysis of the C–ON bond.

It has been proposed that the TS implies that there are several orbital interactions between the nitrogen lone pair (n) and the bonding and anti-bonding orbitals n → σ^*_{O-C}, σ_{O-C} → $\pi^*_{C=O}$, as well as re-hybridization at the N, O, and C atoms, *i.e.*, from sp^3 to sp^2 (Fig. 6). For optimal interactions in the TS (Fig. 6b), the dihedral angles θ_3 and θ_1 need to be as close as possible to 0° to favour the interactions n → σ^*_{O-C} and σ_{O-C} → $\pi^*_{C=O}$. Consequently, the entropic cost to reach a conformation fulfilling these requirements in the TS is expected to be low when these requirements are already observed in the starting materials. Interestingly, in **1a** and **2a**, θ_3 is very close to 0°, meaning that the orbital and bond are already in the required position in the starting materials for efficient n → σ^*_{O-C} interaction in the TS, implying that the TS can be reached without entropic cost.

By taking these statements into account, the *ca.* 20 kJ mol^{-1} decrease in E_a due to the solvent effect observed in **1a** is nicely described by the stabilization of the polar TS, which is enhanced by θ_1 = 24° both in *t*-BuPh and in water (Fig. 7 and Table 3SI†) and is close enough to 0° to generate a low entropic cost. The same stabilization of the TS is expected for **2a**, in sharp contrast to the 4 kJ mol^{-1} decrease in E_a (Table 1)

§§§ The polar effect in the model is given by $(\chi_O - \chi_C)^2$ and assumed to be equivalent to $(\sigma_{I,TEMPO} - \sigma_I)^2$. As electron donating methyl groups are attached to the nitroxyl moiety, it is assumed that $\sigma_{I,TEMPO} = \sigma_{I,H_2NO} = 0.16$. See ref. 37.

¶¶¶ Taking into account footnote §§ and as σ_{RS} was estimated neither reliably nor accurately this data was removed from the correlation set. Nevertheless, k_d is still 14-fold underestimated.

‖‖‖‖ The k_d value of **1b** is clearly an outlier, as it is estimated to be 153-fold stronger than observed. This means that the steric hindrance of $CH(CHO)_2$ is the same as that of the ethyl group. At this stage, we have no rationale for this result.

**** R^2 = 0.94, t = 99.99% for all coefficients, $F_{0.01}$ = 233, and N = 22.

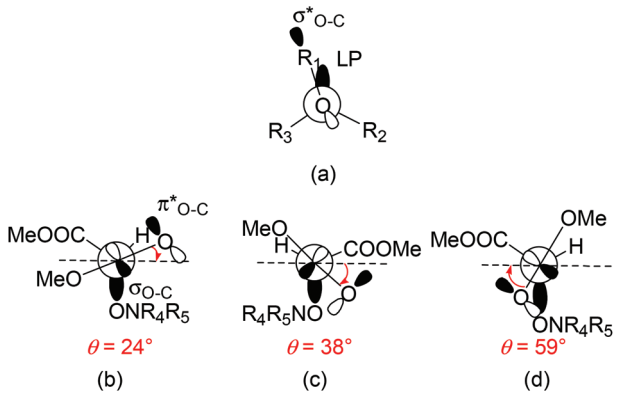

Fig. 7 Newman projections along the N–O bond (a) and along the C–C_1 bond in the alkyl fragments for **1a** both in *t*-BuPh and water (b) and for **2a** in *t*-BuPh (c) and in water (d). The dotted line shows the expected position of the C=O moiety in the TS. The θ values (in red) are the values that the angles have to close by in order to reach the expected conformation in the TS.

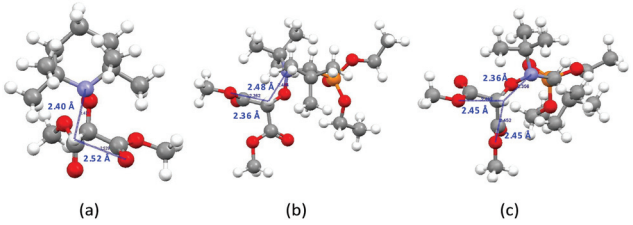

Fig. 8 Calculated IHB interactions for **1a** in toluene and water (a) and for **2a** in toluene (b) and in water (c). The blue lines show IHB.

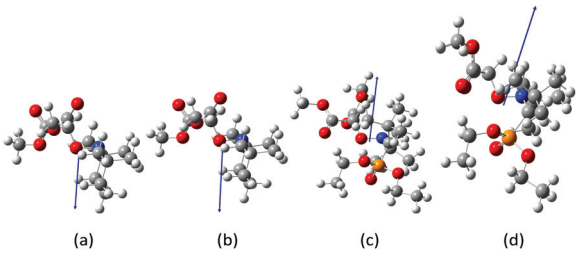

Fig. 9 DFT calculated dipole moments μ for **1a** in toluene (μ = 4.1 D) and water (μ = 4.9 D): (a) and (b) respectively, and for **2a** in toluene (μ = 4.0 D) and water (μ = 6.0 D): (c) and (d), respectively. The blue arrows show the dipole moment vectors.

observed by changing the solvent from *t*-BuPh to water/MeOH. This weaker solvent effect is caused by both a smaller difference in the solvation between TS and alkoxyamine which affords a weaker solvent effect and the entropic cost due to the change in the conformation from **2a** to the TS. First, in *t*-BuPh, the steric strain in **2a** affords a conformation exhibiting a larger θ_1 value than that of **1a**, that is, θ_1 = 38° and θ_1 = 24°, respectively (Table 2). Secondly, in water, θ_1 = 59° is even larger than that in *t*-BuPh which increases the entropic cost to reach the required conformation in the TS. Consequently, gains in energy due to the increase in steric strain and polarity and solvent effects going from **1a** to **2a** and from *t*-BuPh to water/MeOH are almost balanced by the energetic cost due to the solvation and the detrimental changes in conformation in **2a**.

Conformation changes are mainly ruled by 4 effects: (i) stabilizing hyperconjugation, (ii) destabilizing steric strain which has to be minimized, (iii) a dipole moment which has to be minimized in non-polar solvents, and (iv) H-bonding.

A thorough analysis of the geometrical parameters and interactions aforementioned (Table 3SI†) in alkoxyamines **1a** and **2a** shows that, for **1a**, the geometrical parameters (Tables 2SI and 3SI†) and the interactions are the same in water and toluene, whereas for **2a** the geometrical parameters (Tables 2SI and 3SI†) are clearly different in water and toluene, as well as the interactions which differ in number and strength and from those reported for **1a**. 3 hyperconjugation interactions (E = 49 kJ mol^{-1}, Table 3SI†)†††† and 2 IHB interactions‡‡‡‡ (Fig. 8 and Table 3SI†) stabilize **1a** whatever the solvent which means that there are no other conformations providing less steric strain or better hyperconjugation interactions which would overbalance the increase in the dipole moment μ (Fig. 9).

In sharp contrast to **1a**, the conformation of **2a** in water (Fig. 9) exhibits a larger dipole moment (μ = 6.0 D) and greater steric strain (the shortest distances between the carbonyl moieties and methyl groups are 3.11 Å and 3.17 Å, Fig. 8) than the conformation in toluene (μ = 4.0 D, and 3.30 Å and 3.54 Å, Fig. 8). These changes are governed by both the occurrence of hyperconjugation interactions and IHB in toluene – 3 hyperconjugation interactions ((E = 50 kJ mol^{-1}, Table 3SI†)†††† and 2 IHB interactions‡‡‡‡ (Table 3SI† and Fig. 8)) – and those in water – 4 hyperconjugation interactions ((E = 53 kJ mol^{-1}, Table 3SI†)†††† and 3 IHB interactions‡‡‡‡ (Table 3SI† and Fig. 8)).

The solvent effect in **1m**/**1mH+** affords an increase in k_d that is similar to the one observed for **2m**/**2mH+**. As observed for **2m**/**2mH+**, the solvent effect is stronger for **1mH+** than for **1m**, which is likely to be due to the solvation of the counter-anion (Table 1).[31,32]

Experimental section

All of the solvents and reactants for the preparation of the alkoxyamines were used as received. Routine reaction monitoring was performed using silica gel 60 F_{254} TLC plates; the

†††† The sum of the energies with significant hyperconjugation contributions in the ester moieties.

‡‡‡‡ Intramolecular H-bonding is observed between H-acceptors and H-donors for distances smaller than the sum of the van der Waals radii of the atoms involved in IHB: r_H = 1.09 Å, r_N = 1.50 Å and r_O = 1.52 Å. IHB also depends on the valence angle α, *i.e.*, strong IHB is expected when α values that are larger than 150° and weak IHB is expected when α values are smaller than 120°. IHB when α values that are lower than 90° requires strained conformations. See ref. 42 and 43.

spots were visualized upon exposure to UV light and a phosphomolybdic acid solution in EtOH, followed by heating. Purifications were performed on chromatography columns with silica gel grade 60 (230–400 mesh). ^{1}H, ^{13}C, and ^{31}P NMR spectra were recorded in $CDCl_3$ on a 300 or 400 MHz spectrometer. Chemical shifts (δ) were reported in ppm using residual non-deuterated solvents as the internal reference for ^{1}H and ^{13}C-NMR spectra, and 85% H_3PO_4 for ^{31}P-NMR spectra. High-resolution mass spectra (HRMS) were recorded on a SYNAPT G2 HDMS (Waters) spectrometer equipped with a pneumatically assisted atmospheric pressure ionization source (API). Positive mode electrospray ionization was used on the samples: electrospray voltage (ISV): 2800 V; opening voltage (OR): 20 V; nebulizer gas pressure (nitrogen): 800 L h^{-1}. Low resolution mass spectra were recorded on an ion trap AB SCIEX 3200 QTRAP instrument equipped with an electrospray source. The parent ion $[M + H]^+$ is quoted.

General procedure for the preparation of alkoxyamines 1b,c and 2a,c

Lithium diisopropylamine (2 M in THF/hexane), (4.2 ml, 8.33 mmol, 1.1 eq.) was dissolved in THF (30 ml) and cooled to −78 °C. Alkanedione (1.0 g, 7.57 mmol, 1 eq.) was added and the resulting solution was stirred for 45 min prior to the addition of a solution of nitroxide (12.1 mmol, 1.6 eq.) in THF (14 ml). Copper(II) chloride (2.5 g, 18.9 mmol, 2.5 eq.) was added and the reaction mixture was warmed to room temperature. After stirring for another 18 h, the reaction was quenched by the addition of NH_4Cl (aq. sat, 10 ml) and Na_2CO_3 (aq. sat, 10 ml). The aqueous layer was extracted with diethyl ether (3 × 10 ml) and dried over $MgSO_4$. After concentrating under reduced pressure, the residue was purified by column chromatography.

3-((2,2,6,6-Tetramethylpiperidin-1-yl)oxyl)pentane-2,4-dione 1b. Yield of 75%. ^{1}H NMR (400 MHz, $CDCl_3$): δ 4.92 (s, 1H), 2.21 (s, 6H), 1.63–1.26 (m, 6H), 1.19 (s, 6H), 0.96 (s, 6H). ^{13}C NMR (101 MHz, $CDCl_3$): δ 203.9 (2CO), 101.7 (CH), 60.1 (2C), 40.3 ($2CH_2$), 33.1 ($2CH_3$), 27.2 ($2CH_3$), 20.3 ($2CH_3$), 17.0 (CH_2). HRMS (ESI) calc. for $C_{14}H_{26}NO_3$: 256.1907 $[M + H]^+$; found: 256.1908.

Methyl 3-oxo-2((2,2,6,6-tetramethyl piperidine-1-yl))butanoate 1c. Yield of 52%. ^{1}H NMR (400 MHz, $CDCl_3$): δ 4.82 (s, 1H), 3.75 (s, 3H), 2.31 (s, 3H), 1.65–1.37 (m, 4H), 1.36–1.08 (m, 8H), 1.01 (d, J = 16.6 Hz, 6H). ^{13}C NMR (101 MHz, $CDCl_3$): δ 202.9 (CO), 168.4 (COO), 93.6 (CH), 60.3 (C), 60.1 (C), 52.5 (CH_3), 40.2 ($2CH_2$), 33.1 (CH_3), 32.6 (CH_3), 26.6 (CH_3), 20.3 ($2CH_3$), 17.0 (CH_2). HRMS (ESI) calc. for $C_{14}H_{26}NO_4^+$: 272.1856 $[M + H]^+$; found: 272.1857.

Dimethyl 2-((*tert*-butyl(1-(diethoxyphosphoryl)-2,2-dimethylpropyl)amino)oxy)malonate 2a. Yield of 25%. ^{1}H NMR (400 MHz, $CDCl_3$): δ 5.10 (s, 1H), 4.45–4.36 (m, 1H), 4.34–4.24 (m, 1H), 4.11–4.01 (m, 1H), 3.99–3.91 (m, 1H), 3.76 (s, 6H), 3.27 (d, J = 25.5 Hz, 1H), 1.36–1.24 (m, 6H), 1.13 (s, 9H), 1.09 (s, 9H). ^{31}P NMR (162 MHz, $CDCl_3$) δ 24.45. ^{13}C NMR (101 MHz, $CDCl_3$): δ 167.7 (COO), 166.7 (COO), 86.0 (CH), 69.4 (CH, d, J = 138.7 Hz), 62.7 (C), 62.5 (CH_2, d, J = 6.2 Hz), 59.0 (CH_2, d, J = 7.3 Hz), 52.7 (CH_3), 52.6 (CH_3), 35.7 (C, d, J = 5.4 Hz), 29.4 ($3CH_3$, d, J = 5.8 Hz), 27.9 ($3CH_3$), 16.8 (CH_3, d, J = 5.7 Hz), 16.4 (CH_3, d, J = 6.8 Hz). HRMS (ESI) calc. for $C_{18}H_{37}NO_8P^+$: 426.2251 $[M + H]^+$; found: 426.2252.

Methyl 2-((*tert*-butyl(1-(diethoxyphosphoryl)-2,2-dimethylpropyl)amino)oxy)-3-oxobutanoate 2c. Yield of 23% as an oil. For the minor isomer: ^{1}H NMR (400 MHz, $CDCl_3$): δ 4.98 (s, 1H), 4.35 (dd, J = 14.9, 7.4 Hz, 2H), 4.11–3.92 (m, 2H), 3.73 (s, 3H), 3.27 (d, J = 25.9 Hz, 1H), 2.46 (s, 3H), 1.31 (dt, J = 15.8, 6.3 Hz, 7H), 1.14 (s, 9H), 1.07 (s, 9H). ^{31}P NMR (162 MHz, $CDCl_3$): δ 24.81. ^{13}C NMR (101 MHz, $CDCl_3$): δ 202.9 (CO), 168.4 (COO), 93.6 (CH), 68.9 (CH, d, J = 137.7 Hz), 62.7 (C), 62.1 (CH_2, d, J = 6.6 Hz), 59.5 (CH_2, d, J = 7.5 Hz), 52.6 (CH_3), 35.8 (C, d, J = 5.9 Hz), 29.4 ($3CH_3$), 28.2 ($3CH_3$), 26.9 (CH_3), 16.6 (CH_3, d, J = 6.3 Hz), 16.3 (CH_3, d, J = 6.6 Hz). HRMS (ESI) calc. for $C_{18}H_{37}NO_7P^+$: 410.2302 $[M + H]^+$; found: 410.2299. For the major isomer: ^{1}H NMR (400 MHz, $CDCl_3$): δ 5.10 (s, 1H), 4.47–4.36 (m, 1H), 4.34–4.24 (m, 1H), 4.13–4.02 (m, 1H), 4.00–3.91 (m, 1H), 3.74 (s, 3H), 3.24 (d, J = 25.1 Hz, 1H), 2.26 (s, 3H), 1.32 (t, J = 7.2 Hz, 3H), 1.28 (t, J = 7.1 Hz, 3H), 1.10 (s, 9H), 1.06 (s, 9H). ^{31}P NMR (162 MHz, $CDCl_3$): δ 24.70. ^{13}C NMR (101 MHz, $CDCl_3$): δ 201.4 (CO), 167.4 (COO), 94.3 (CH), 69.3 (CH, d, J = 138.4 Hz), 62.8 (C), 62.4 (CH_2, d, J = 6.1 Hz), 59.1 (CH_2, d, J = 7.3 Hz), 52.6 (CH_3), 35.8 (C, d, J = 5.9 Hz), 29.0 ($3CH_3$), 28.1 ($3CH_3$), 27.2 (CH_3), 16.9 (CH_3, d, J = 5.4 Hz), 16.4 (CH3, d, J = 6.7 Hz). HRMS (ESI) calc. for $C_{18}H_{37}NO_7P^+$: 410.2302 $[M + H]^+$; found: 410.2298.

2-Phenyl-2-((2,2,6,6-tetramethylpiperidin-1-yl)oxyl)acetaldehyde 1g. 2-Phenyl-2-((2,2,6,6-tetramethylpiperidin-1-yl)oxyl)ethanol (100 mg, 0.36 mmol, 1 eq.) was dissolved in dichloromethane (3 ml) and cooled to 0 °C. Tetrapropylammonium perruthenate (TPAP, 13 mg, 36 μmol, 0.1 eq.) was added and the resulting solution was stirred until it turned black prior to the addition of a solution of *N*-methyl morpholine oxide (NMO, 130 mg, 1.08 mmol, 3 eq.). After stirring for another 2 h, the reaction was quenched by the addition of Na_2CO_3 (aq. sat, 3 ml). The aqueous layer was extracted with dichloromethane (3 × 5 ml) and dried over $MgSO_4$. After concentrating under reduced pressure, the residue was purified by column chromatography (56 mg, 56%). ^{1}H NMR (400 MHz, $CDCl_3$) δ 9.66 (d, J = 3.8 Hz, 1H), 7.41–7.29 (m, 5H), 5.09 (d, J = 3.8 Hz, 1H), 1.63–1.33 (m, 6H), 1.27 (s, 3H), 1.20 (s, 3H), 1.14 (s, 3H), 0.87 (s, 3H). ^{13}C NMR (101 MHz, $CDCl_3$) δ 199.1 (CO), 135.4 (CH), 128.7 ($2CH_2$), 128.2 (CH_2), 127.0 ($2CH_2$), 93.1 (CH), 60.2 (C), 59.9 (C), 40.0 ($2CH_2$), 33.9 (CH_3), 33.4 (CH_3), 20.5 (CH_3), 20.2 (CH_3), 17.0 (CH_2). HRMS (ESI) calc. for $C_{17}H_{26}NO_2^+$: 276.1958 $[M + H]^+$; found: 276.1959.

4-[1-(2,2,6,6-Tetramethylpiperidin-1-yloxy)-ethyl]-pirydine 1m. In an open flask, $MnCl_2$ (84 mg, 0.67 mmol, 0.1 eq.) was added to a stirred solution of salen ligand (180 mg, 0.67 mmol, 0.1 eq.) in isopropanol (10 mL). After 30 min of stirring at room temperature, a solution of TEMPO (1.56 mg, 10 mmol, 1.5 eq.) and 4-vinylpyridine (700 mg, 6.66 mmol, 1 eq.) in isopropanol (10 mL) was added, then solid $NaBH_4$ (490 mg, 5.55 mmol, 1 eq.) was added in small portions. The mixture was stirred for 24 h at room temperature. The solvent

was evaporated to give the crude product. After concentrating under reduced pressure, the residue was purified by column chromatography to afford 544 mg of **1m** (32%). ^{1}H NMR (400 MHz, $CDCl_3$) δ 8.53 (d, J = 6.0 Hz, 2H), 7.23 (d, J = 6.0 Hz, 2H), 4.77 (q, J = 6.7 Hz, 1H), 1.62–1.35 (m, 9H), 1.27 (s, 3H), 1.16 (s, 3H), 1.04 (s, 3H), 0.69 (s, 3H). ^{13}C NMR (75 MHz, $CDCl_3$) δ 153.99 (C), 149.19 (2CH), 121.12 (2CH), 81.65 (CH), 59.39 (2C), 39.98 ($4CH_3$), 22.93 ($3CH_2$), 16.81 (CH_3). HRMS (ESI) calc. for $C_{16}H_{27}N_2O^+$: 263.2118 $[M + H]^+$; found: 263.2119.

Kinetic measurements

The homolysis rate constants k_d were measured by EPR[27] as previously reported and were given by eqn (7). Air was used as the alkyl radical scavenger for the EPR experiments. Activation energies E_a were estimated using eqn (8) and the average frequency factor $A = 2.4 \times 10^{14}$ s^{-1}. Values of k_d and E_a are listed in Table 1.

$$\ln \frac{[\text{nitroxide}]_\infty - [\text{nitroxide}]_t}{[\text{nitroxide}]_\infty} = -k_d \cdot t \quad (7)$$

$$E_a = 8.314 \cdot T \cdot \ln \frac{2.4 \times 10^{14}}{k_d} \quad (8)$$

Conclusion

The Bond Dissociation Energy (BDE) is described by the sum of enthalpic and polar terms given in eqn (5) as proposed by Pauling.[38–40] Often, and especially concerning the C–ON bond homolysis in alkoxyamines, it is assumed that the E_a for homolysis and BDE are very similar. Consequently, E_a or $\log k_d$ should be given by a multi-parameter relationship based on parameters describing stabilization and steric effects by a linear model and on a parabolic model describing the polar effect. The results described above for **1**-based alkoxyamines show that the linear relationship using a parabolic model for the polar effect (eqn (6) and Fig. 5) is able to account for all of the data, in sharp contrast to the simple linear multi-parameter model (Fig. 2 and eqn (2)). Therefore, it should also be applied to **2**-based alkoxyamines. However, it is truly needed when very strong EWGs are on the alkyl fragment, affording χ_C values that are larger than χ_O values. The main drawback for the use of a parabolic model is that the electrical Hammett constant $\sigma_{I,nitroxide}$ of the nitroxyl fragment has to be determined. As a rule of thumb, one may assume that it should be used when the alkyl and nitroxyl fragments carry strong EWGs and EDGs, respectively.

In this work, a striking 1500-fold increase in k_d due to the solvent effect is also reported. As far as we know, it is the largest solvent effect reported for alkoxyamines at the present time. It is likely to be due to the stabilization in the TS and the impact of this effect depends a lot on the favoured conformation of the alkyl fragment. This conformation is ruled by a subtle interplay of the occurrence of hyperconjugation, steric strain, dipole moments and H-bonding.

This improved description of the polar and solvent effects in alkoxyamine C–ON bond homolysis is important and needed in order to design new alkoxyamines suitable for more efficient NMP in various conditions,[9,16] to develop smart materials,[3–6] or to favour new applications in biology.[8]

Acknowledgements

The authors thank Aix-Marseille University and the CNRS for financial support. ANR granted funding for this project (ANR-14-CE16-0023-01). PN thanks the Ministere de la Recherche du Gabon and Campus France for the Ph.D. grant. The authors thank the RENARD network for the EPR platform.

Notes and references

1 G. Audran, P. Brémond and S. R. A. Marque, *Chem. Commun.*, 2014, **50**(59), 7921–7928.
2 C. Yuan, M. Z. Rong, M. Q. Zhang, Z. P. Zhang and Y. C. Yuan, *Chem. Mater.*, 2011, **23**, 5076–5081.
3 Z. P. Zhang, M. Z. Rong, M. Q. Zhang and C. Yuan, *Polym. Chem.*, 2013, **4**, 4648–4654.
4 B. Schulte, M. Tsotsalas, M. Becker, A. Studer and L. De Cola, *Angew. Chem., Int. Ed.*, 2010, **49**, 6881–6884.
5 R. K. Roy, C. X. Laure, D. Fischer-Krauser, L. Charles and J.-F. C. O. Lutz, *Chem. Commun.*, 2015, **51**, 15677–15680.
6 R. K. Roy, A. Meszynska, C. E. Laure, L. Charles, C. Verchin and J.-F. C. O. Lutz, *Nat. Commun.*, 2015, **6**, 1–8.
7 D. Moncelet, P. Voisin, N. Koonjoo, V. Bouchaud, P. Massot, E. Parzy, G. Audran, J.-M. Franconi, E. Thiaudière, S. R. A. Marque, P. Brémond and P. Mellet, *Mol. Pharmaceutics*, 2014, **11**, 2412–2419.
8 G. Audran, P. Brémond, J.-M. Franconi, S. R. A. Marque, P. Massot, P. Mellet, E. Parzy and E. Thiaudière, *Org. Biomol. Chem.*, 2014, **12**, 719–723.
9 J. Nicolas, Y. Guillaneuf, C. Lefay, D. Bertin, D. Gigmes and B. Charleux, *Prog. Polym. Sci.*, 2013, **38**, 63–235.
10 Registration, Evaluation, Authorisation, and Restriction of Chemical Substances (REACH), EC, 1907/2006, http://eur.lex.europa.eu/LexUriServ/LexUriServ.do?uri=CELEX:32006R1907:en:NOT, accessed Sept 19, 2013.
11 J. L. Hodgson, C.-Y. Lin, M. L. Coote, S. R. A. Marque and K. Matyjaszewski, *Macromolecules*, 2010, **43**(8), 3728–3743.
12 C. Y. Lin, S. R. A. Marque, K. Matyjaszewski and M. L. Coote, *Macromolecules*, 2011, **44**(19), 7568–7583.
13 S. Marque, *J. Org. Chem.*, 2003, **68**, 7582–7590.
14 H. Fischer, A. Kramer, S. R. A. Marque and P. Nesvadba, *Macromolecules*, 2005, **38**, 9974–9984.
15 D. Bertin, D. Gigmes, S. R. A. Marque and P. Tordo, *Macromolecules*, 2005, **38**, 2638–2650.
16 D. Bertin, D. Gigmes, S. R. A. Marque and P. Tordo, *Chem. Soc. Rev.*, 2011, **40**, 2189.

17 D. Bertin, P.-E. Dufils, I. Durand, D. Gigmes, B. Giovanetti, Y. Guillaneuf, S. R. A. Marque, T. Phan and P. Tordo, *Macromol. Chem. Phys.*, 2008, **209**, 220–224.
18 E. Guegain, V. Delplace, T. Trimaille, D. Gigmes, D. Siri, S. R. A. Marque, Y. Guillaneuf and J. Nicolas, *Polym. Chem.*, 2015, **6**, 5693–5704.
19 K. Molawi, T. Schulte, K. O. Siegenthaler, C. Wetter and A. Studer, *Chem. – Eur. J.*, 2005, **11**, 2335–2350.
20 P. Brémond, A. Koïta, S. R. A. Marque, V. Pesce, V. Roubaud and D. Siri, *Org. Lett.*, 2012, **14**(1), 358–361.
21 P. Brémond and S. R. A. Marque, *Chem. Commun.*, 2011, **47**(14), 4291–4293.
22 This procedure is derived from C. Wetter, K. Jantos, K. Woithe and A. Studer, *Org. Lett.*, 2003, **5**(16), 2899.
23 B.-L. Chen, Y.-J. Wang, H. Guo and G.-Y. Zeng, *Eur. J. Med. Chem.*, 2016, **109**, 199–205.
24 K. Matyjaszewski, B. E. Woodworth, X. Zhang, S. G. Gaynor and Z. Metzner, *Macromolecules*, 1998, **31**, 5955.
25 A. Prechter and M. R. Heinrich, *Eur. J. Org. Chem.*, 2013, 5585–5589.
26 D. Bianchi, P. Cesti and E. Battistel, *J. Org. Chem.*, 1988, **53**, 5531.
27 S. Marque, C. Le Mercier, P. Tordo and H. Fischer, *Macromolecules*, 2000, **33**(12), 4403–4410.
28 E. Megiel, A. Kaim and M. K. Cyrański, *J. Phys. Org. Chem.*, 2010, **23**, 1146–1154.
29 A. Goto, Y. Kwak, C. Yoshikawa, Y. Tsujii, Y. Sugiura and T. Fukuda, *Macromolecules*, 2002, **35**, 3520.
30 G. Audran, P. Brémond, S. R. A. Marque and T. Yamasaki, *J. Org. Chem.*, 2016, **81**, 1981–1988.
31 G. Audran, P. Brémond, S. R. A. Marque and G. Obame, *J. Org. Chem.*, 2013, **78**, 7754–7757.
32 G. Audran, P. Brémond, S. R. A. Marque and G. Obame, *Polym. Chem.*, 2012, **3**, 2901–2908.
33 M. Charton, *Top. Curr. Chem.*, 1983, 58–91.
34 J. J. Brocks, H. D. Beckhaus and A. Beckwith, *J. Org. Chem.*, 1998, **63**, 1935–1943.
35 F. A. Neugebauer, Carbon Radicals with Conjugated π-System, in *Magnetic Properties of Free Radicals*, ed. H. Fischer, Landolt-Börnstein, Group II, Springer-Verlag, Berlin, 2002, vol. 26.
36 C. Hansch, A. Leo and R. W. Taft, *Chem. Rev.*, 1991, **91**, 165–195.
37 M. Charton, *Prog. Phys. Org. Chem.*, 1981, **13**, 119–251.
38 L. Pauling, *The Nature of the Chemical Bond*, Cornell University Press, Ithaca, NY, 1960.
39 B. P. Roberts, *J. Chem. Soc., Perkin Trans. 2*, 1996, 2719–2725.
40 A. A. Zavitsas, Thermochemistry and Hydrogen Transfer Kinetics, in *Encyclopedia of Radicals in Chemistry, Biology, and Materials*, ed. C. Chatgilialoglu and A. Studer, Wiley, Chichester, U.K., 2012, pp. 81–106.
41 J. Tomasi, B. Mennucci and R. Cammi, *Chem. Rev.*, 2005, **105**, 2999–3093.
42 R. S. Rowland and R. Taylor, *J. Phys. Chem.*, 1996, **100**, 7384–7391.
43 G. A. Jeffrey and W. Saenger, *Hydrogen Bonding in Biological Structures*, Springer, Berlin, Heidelberg, 1994.

